Journal of Theoretical Biology 424 (2017) 37–48

Contents lists available at ScienceDirect

Journal of Theoretical Biology

journal homepage: www.elsevier.com/locate/jtbi

Bidirectionality from cargo thermal fluctuations in motor-mediated transport

Christopher E. Miles*, James P. Keener

University of Utah, Department of Mathematics, 155 S 1400 E, room 233, Salt Lake City, UT 84112-0090, United States

ARTICLE INFO

Article history:
Received 10 December 2016
Revised 26 April 2017
Accepted 29 April 2017
Available online 1 May 2017

Keywords:
Molecular motors
Intracellular transport
Diffusion
Stochastic processes
Mean first passage times

ABSTRACT

Molecular motor proteins serve as an essential component of intracellular transport by generating forces to haul cargoes along cytoskeletal filaments. Two species of motors that are directed oppositely (e.g. kinesin, dynein) can be attached to the same cargo, which is known to produce bidirectional net motion. Although previous work focuses on the motor number as the driving noise source for switching, we propose an alternative mechanism: cargo diffusion. A mean-field mathematical model of mechanical interactions of two populations of molecular motors with cargo thermal fluctuations (diffusion) is presented to study this phenomenon. The delayed response of a motor to fluctuations in the cargo velocity is quantified, allowing for the reduction of the full model a single "characteristic distance", a proxy for the net force on the cargo. The system is then found to be metastable, with switching exclusively due to cargo diffusion between distinct directional transport states. The time to switch between these states is then investigated using a mean first passage time analysis. The switching time is found to be non-monotonic in the drag of the cargo, providing an experimental test of the theory.

1. Introduction

Active transport is a key component of cellular function due to the compartmental nature of cellular machinery. This transport is achieved through the use of molecular motor proteins, which undergo a series of conformational changes to walk along cytoskeletal filaments and generate forces to haul cargoes (Howard, 2001). The transport of a single cargo can often involve two families of motors that are directed oppositely. For instance, kinesin, which primarily walks in the positive direction of a microtubule, and dynein, primarily in the negative direction, can be attached to the same cargo. Another possibility is that two populations of the same family of kinesin motor can be attached to a cargo but walk along oppositely oriented microtubule tracks (Osunbayo et al., 2015). This phenomenon of opposing motor populations is observed for a wide variety of cargoes: mRNA particles, virus particles, endosomes, and lipid droplets (Hendricks et al., 2010; Kunwar et al., 2008). Although both families of motors are exerting forces on the cargo in opposite directions, the net motion of cargo transport is able to switch. That is, the cargo spends periods of time with a net positive, negative, and zero velocity (denoted a pause state), the overall motion of which is denoted *bidirectional transport* (Hancock, 2014). This intuitively inefficient transport phenomenon is thought to serve a role in pattern formation (Brooks and Bressloff, 2016) or spatially uniform cargo delivery (Bressloff and Levien, 2015). However, this work focuses on the *mechanism* of switching. That is, the distinct switching between directions suggests the existence of a mechanism of *cooperation* between the motor families, which has been explored previously from both experimental and theoretical perspectives.

The role of external influences in the cooperation mechanism remains unclear. A number of studies have identified regulators of kinesin and dynein (Fu and Holzbaur, 2014). For instance, LIS1 and NudE have been found to modulate dynein's force production capabilities (McKenney et al., 2010). In Shojania Feizabadi et al. (2015), the authors found that the microtubule itself can regulate kinesin force production. However, the necessity of these external regulators for motor coordination in bidirectional transport remains unestablished. The alternative hypothesis relies on the notion that the coordination is a product of the mechanical interactions of the motors with the cargo, denoted a *tug-of-war* scenario.

The tug-of-war hypothesis has also been investigated from a theoretical and experimental perspective. The authors in Müller et al. (2008) formulate the most notable mathematical model capable of producing bidirectionality. In the model, the motors share the load equally. This assumption is not always invoked in later mathematical models. For instance, Kunwar et al. (2011) performs stochastic simulations of unequally distributed motors. However,

* Corresponding author.
E-mail address: miles@math.utah.edu (C.E. Miles).

http://dx.doi.org/10.1016/j.jtbi.2017.04.032
0022-5193/

these authors compare the results of the stochastic simulation with experiments and conclude that switching statistics do not match as the number of motors varies. In Soppina et al. (2009), another mathematical model is proposed where the two motor populations are required to be asymmetric. That is, the two opposing motor populations must have different force generating properties to break symmetry. Lipowsky et al. (2010); 2006) also provide noteworthy mathematical models, thinking of motor transport as a "rubber-band"-like process and find rich dynamics. Although not specifically about tug-of-war, motor population models such as the Huxley crossbridge model (Huxley, 1957; Keener and Sneyd, 2008) use force-velocity relationships for the motor populations. However, since this analysis is a steady-state analysis, it is difficult to infer dynamics, which we address in our model. In Bouzat (2016), the authors reexamine the mathematical model of Kunwar et al. (2011) and stress the importance of cargo diffusion for the model to produce the right behavior, specifically pointing out the issue of relating steady-state force-velocity curves to dynamics. An asymptotic analysis of a model bearing many similarities to our proposed model (but still with discrete motor number) can be found in McKinley et al. (2012). The authors include cargo diffusion in a stochastic differentialequation description and note that motor dynamics slow compared to fast fluctuations in the cargo velocity, which ultimately is an important ingredient of our work.

In this work, we present a new tug-of-war model of bidirectional motor-mediated transport. Our proposed model contains fundamentally different essential components than previous work. Broadly, the proposed model is a mean-field model with unequally distributed load. This differs from previous discrete motor, unequal load descriptions and therefore requires a different source of noise to induce switching. By examining the force generation of bound motors, we quantify the delayed response to instantaneous changes in the cargo velocity. We make an approximation (and justify numerically) that this delay structure extends beyond the scope of only bound motors, allowing for the use of a force-velocity relationship to study the full system. This reduction leads to a system of two "characteristic distances", one for each motor population. By symmetry, this two-variable system is collapsed to a single dimension which is found to be metastable, with two states corresponding to positive and negative net velocities, or bidirectional motion. The noise that drives switching between these two states is due to cargo diffusion (thermal fluctuations), an aspect of this process previously noticed but under-emphasized until recently (Bouzat, 2016).

Previous work has indeed illustrated the significance of motor number fluctuations (Nadrowski et al., 2004). However, in this present work, we choose to use a mean-field model to emphasize the lack of necessity of discrete motor number for bidirectionality. Our proposed model still incorporates binding and unbinding dynamics and therefore has the same *mean* behavior as a discrete motor model, but lacks the noise associated with discrete events. The only remaining noise source is then cargo diffusion, which we show to be sufficient for bidirectionality. The difference in magnitudes between the fluctuations due to motor number and cargo diffusion is difficult to quantify due to the fundamental difference in structure. In Guérin et al. (2011a), the authors find that motor number fluctuations can result in an effective diffusion when the number of motors involved in transport is large.

A characteristic quantity in validating bidirectional transport models is the reversal or switching time of the system: the time between runs of each direction. In our model, the correlation structure of the effect of noise on each population allows for the reduction to an invariant manifold and consequently, a one dimensional mean first passage time problem in a double-well potential. Classical tools can then be used to numerically solve and analytically approximate the corresponding boundary value problem. The switching time is considered as a function of the cargo drag coefficient, which leads to complex behavior as the wells steepen but diffusion strengthens as the drag decreases. Ultimately, the mean switching time is found to be non-monotonic in the cargo drag coefficient, a feature not expected for switching due to motor dynamics. This non-monotonicity provides an experimental test to validate (or refute) our diffusion-driven switching hypothesis.

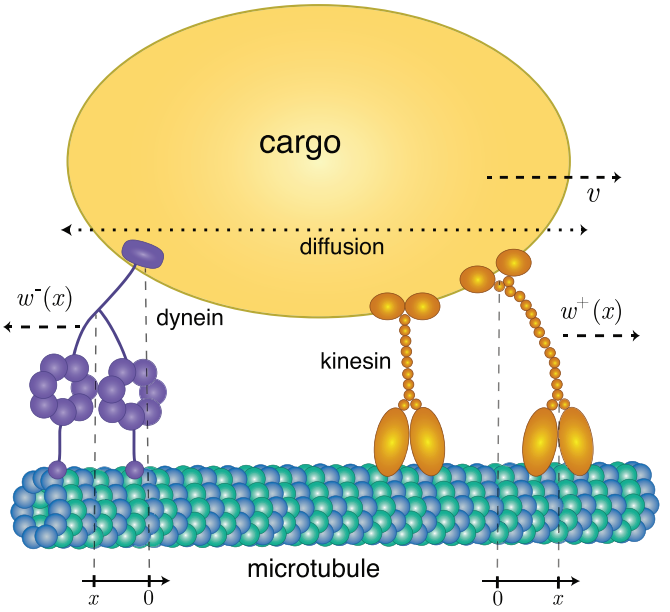

Fig. 1. A diagram of the mean-field model setup. The quantity, x, denoting the distance a motor is stretched is always measured with respect to the orientation of the microtubule.

2. Methods

2.1. Model formulation

Consider a cargo being pulled by two different populations of motors, denoted + and −. Let $m^{\pm}(x, t)$ be the density of type + or − motors at time t and stretched from their unstretched distance x units. The + or − labeling of the motor families denotes their preferred directionality. That is, m^+ corresponds to the density of motors preferring to walk in the positive direction (e.g. kinesin) and m^- the density of motors preferring to walk in the negative direction (e.g. dynein) as seen in Fig. 1. Although the negatively oriented motors are depicted as dynein in the figure, this need not be the case. The negatively oriented motors could be, for instance, another set of kinesin motors on an opposing microtubule. The framework presented is sufficiently general to accommodate both. The evolution of each motor population is then described by

$$\frac{\partial m^{\pm}}{\partial t} + \underbrace{\frac{\partial}{\partial x}\left\{\left[w^{\pm}(x) - v(t)\right]m^{\pm}\right\}}_{\text{stepping}} = \underbrace{\left(M^{\pm} - \int_{-\infty}^{\infty} m^{\pm}(x,t)\,\mathrm{d}x\right)\Omega^{\pm}_{\text{on}}(x)}_{\text{binding}} - \underbrace{\Omega^{\pm}_{\text{off}}(x)m^{\pm}(x,t)}_{\text{unbinding}}. \tag{1}$$

Although (1) appears as only one equation, m^+ and m^- each have their own equation that are structurally identical but may contain different parameters or functional forms. The quantity x, describing the distance the motor is stretched from its unstretched

displacement is always measured with respect to the microtubule, even though each motor type walks in a different direction, see Fig. 1. This choice of frame of reference is convenient, as it causes the two equations to be structurally identical (as opposed to having to reverse the sign of v).

It is worth noting that this PDE has been studied in other contexts and is referred to as the Lacker–Peskin PDE (Srinivasan and Walcott, 2009), which is an extension of the Huxley crossbridge model (Huxley, 1957; Keener and Sneyd, 2008). In that literature, the particular form of the PDE is derived from the limit of a large number of discrete binding sites or a large number of motors. However, in the present context, it is well established that the number of motors is quite small (Hendricks et al., 2010; Rai et al., 2013), hence a different interpretation for the mean-field model must be taken. If $M = 1$, Eq. (1) is a Chapman–Kolmogorov equation, corresponding to the behavior of a single motor and describes the probability of finding a motor stretched distance at x at time t. This process is inherently random by the stochastic nature of the binding dynamics, which is entirely accounted for in the binding and unbinding terms of the mean-field equation.

Cargo mediated transport is a multi-motor phenomenon, and consequently, we are interested in the behavior of an ensemble of motors. However, we point out the observation that (ignoring crowding effects) the motors interact solely through the cargo. For this reason, the motors can be treated as acting identically and independently, and hence, a mean-field model, which can be thought of as a rescaling of the Chapman–Kolmogorov equation for a single motor, is applicable. To elaborate, we can regard $m(x, t)$ as the *expected* (or mean, hence the name *mean-field*) number of motors bound at a given x and t. By construction, $0 \leq \int m\,dx \leq M$, and therefore the interpretation of M is a maximum number of motors bound. Thus, we have effectively averaged over the stochasticity in the binding dynamics to study a mean-field description of motor ensembles.

Before describing, in detail, each term in (1), we state a driving assumption for several of the functional forms appearing in the equation. The force generated due to the linker stretching is assumed to be Hookean, that is force $\sim kx$, where k is the spring constant or stiffness of the motor linker attachment to the cargo. The force-displacement curve of molecular motors has been studied experimentally (Kawaguchi et al., 2003; Lindemann and Hunt, 2003) and, although not perfectly linear, seems to be well-approximated by this assumption.

We now discuss each term of the equation in more detail. Broadly, the motor population can change in three ways: motors stepping (walking), binding or unbinding.

1. **stepping**: We assume that the rate of stepping for motors is dependent on the force exerted on the motor, typically characterized by a force-velocity curve. The force on the motor is generated by the linker displacement x in a Hookean manner, $F = kx$. Consequently, the walking rate of a motor is more naturally thought of as a *displacement*-velocity relationship, which is qualitatively the same as the force-velocity curve by the linearity of the force generation. Denote this displacement-velocity curve by $w(x)$ and take it to be of the linear form

$$w(x) := -ax + b, \tag{2}$$

where $a > 0$. At $x = 0$, which corresponds to the motor being unstretched, the motor walks with some velocity b. For the $+$ directed motor, for instance, $b > 0$. As the motor walks farther from its unstretched position ($x > 0$), the force exerted on it causes the velocity to decrease until it eventually stalls at $x_{\text{stall}} := b/a$. If $x < 0$, that is, the cargo is ahead in the direction the motor seeks to walk, the velocity is assumed to be greater as the linker exerts a force in the direction of motion of the motor. If $x > x_{\text{stall}}$, then the force exerted by the linker is greater than the stall force, meaning the motor moves opposite its preferred direction.

Force-velocity relationships have been qualitatively observed experimentally for kinesin (Gennerich et al., 2007; Kunwar et al., 2008) and dynein (Belyy et al., 2014). One notable observation is a dramatic difference in behavior between motors in high ATP environments (Carter and Cross, 2005; Visscher et al., 1999) and ATP starved motors (Gross et al., 2007; Mitchell and Lee, 2009). For this work, we assume the motors operate with sufficient ATP. The force-velocity curve is visibly nonlinear, with main deviation from linearity occurring at superstall forces, where motors velocities become negative (as in this model), but with much smaller magnitude. Motors operating with an assisting force ($x < 0$ in this model) also appear to operate with sub-linear velocities. For this reason, a sigmoidal form (due to its saturating behavior) is deemed appropriate and used in a number of other modeling papers (Bouzat, 2016; Kunwar et al., 2011; McKinley et al., 2012; Müller et al., 2008). However, in this work, we assume that motors operate in a regime of the force-velocity curve that can be approximated by its linearization. This assumption is explored and discussed further in Section 3.1.

2. **binding**: The functional form of the binding term is set to be

$$\Omega_{\text{on}}(x) := k_{\text{on}}\ \delta(x),$$

where k_{on} is the constant describing the rate of binding of a molecular motor to the cargo. The $\delta(x)$ functional form corresponds to the assumption that motors are initially unstretched ($x = 0$) when they bind, thus only binding at $x = 0$. That is, the motors only bind in a non-force-producing state. This assumption can be relaxed (and is for later numerical simulations) to a Gaussian approximation of the delta function.

3. **unbinding**: The unbinding rate of molecular motors has experimentally been found to be related to the force exerted on them (Kawaguchi et al., 2003; Kunwar et al., 2011), however the nature of this dependency is complex and varies from motor to motor. Dynein is found to a have a catch-bond behavior (Kunwar et al., 2011; Nicholas et al., 2015). Both kinesin (Andreasson et al., 2015) and dynein (Nicholas et al., 2015) have been observed to have asymmetric force dependence in their unbinding.

Due to the complexity and variation in unbinding dependence, we take the simplest form that still behaves in a way that qualitatively matches experimental results, which is

$$\Omega_{\text{off}}(x) = k_{\text{off}}\ \exp\left\{\frac{k|x|}{F_D}\right\},$$

where again, the force exerted is assumed to be Hookean ($\sim kx$), and independent of direction (hence the absolute value). F_D is a characteristic force fit to experimental observations, and k_{off} is the unstretched detachment rate. This form is often referred to as Bell's Law, which is known to need corrections in some scenarios (Walcott, 2008). The overall behavior of this function establishes that motors detach at a faster rate the farther they are stretched due to the force exerted on their microtubule binding sites.

This functional form (or similar) has been used in other motor population models (Srinivasan and Walcott, 2009; Walcott, 2008). In Kunwar et al. (2011), the authors account for the stalling of motors and the catch-bond behavior of dynein by taking a non-monotonic dependence on the force. In our unbinding rate, neither the catch-bond behavior nor is the asymmetric dependence on force is included. The consequence of excluding these phenomena is purely quantitative, as they are not

dramatic enough effects (in the regimes that motors operate for transport) to produce a qualitative effect in our model.

It is also worth noting that Ω_{off} and Ω_{on} have different units, as the off-rate is multiplied by m, a motor density and the on-rate is multiplied by a total number of motors $\int m\,dx$.

We then can define the average force exerted by each motor population, recalling the assumption of a Hookean force,

$$F^{\pm}(t) := \int_{-\infty}^{\infty} k^{\pm} x m^{\pm}(x,t)\,dx. \tag{3}$$

This time-varying quantity requires knowledge of the full density of motors $m(x, t)$, which makes it difficult to study directly.

2.2. Steady-state analysis

This time-dependent force, described by (3) is difficult to compute in practice, so we turn our attention to the steady-state force. We consider the steady state ($dm^{\pm}/dt = 0$) and behavior of (1) with some steady-state velocity $\tilde{v}$, which leads to the pair of equations for the steady state densities $\tilde{m}^{\pm}$

$$\frac{\partial}{\partial x}\left\{\left[w^{\pm}(x) - \tilde{v}\right]\tilde{m}^{\pm}\right\} = \left(M^{\pm} - \int_{-\infty}^{\infty} \tilde{m}^{\pm}(x)\,dx\right)\Omega_{\text{on}}^{\pm}(x) - \Omega_{\text{off}}^{\pm}(x)\tilde{m}^{\pm}(x). \tag{4}$$

Exploiting the linearity of (4), along with the partitioning nature of the delta function, (4) can be solved analytically, resulting in a solution with an integrable singularity at the stall distance dependent on the velocity

$$x_{\text{stall}} := \frac{b - \tilde{v}}{a}.$$

For details of this calculation, see *Supplementary Section S1*. This allows us to define the steady state force exerted by each population of motor

$$\tilde{F}^{\pm}(\tilde{v}) := \int_{-\infty}^{\infty} k^{\pm} x \tilde{m}(x;\tilde{v})\,dx, \tag{5}$$

where we parameterize this force as a function of the steady state cargo velocity $\tilde{v}$ which appears in (4).

We now need an equation governing the cargo velocity, which is determined by the forces exerted on the cargo

$$\mathcal{M}\dot{v} + \gamma v = \sqrt{2\gamma k_B T}\xi(t) + \text{forces exerted by motors}. \tag{6}$$

In (6), $\mathcal{M}$ is the mass of the cargo, γ is the drag coefficient of the cargo and $\xi(t)$ is the white-noise process due to thermal fluctuations (diffusion) of the cargo which satisfies $\langle \xi(t)\xi(\tau)\rangle = \delta(t-\tau)$. The magnitude of these fluctuations is determined by the fluctuation-dissipation theorem (Gardiner, 2009).

2.3. Forces exerted by motors

A perhaps natural choice for the force terms in (6) could be the steady-state force, $\tilde{F}^{\pm}(v)$, found in (5). The use of a *force-velocity* relationship (which $\tilde{F}$ is) to study motors has a long history (e.g. Huxley (1957)) but there is a problem with this choice. Although v is changing instantaneously, the position of the cargo is not. The forces exerted by the motors are due to stretching of the linker (determined by their displacement), which does *not* change instantaneously as the velocity changes. In other words, it is impossible to completely infer *dynamics* from a *steady-state* force-velocity relationship. Thus, parameterizing the force with time-varying velocity would not produce the physical behavior we desire. For this reason, we turn to a simpler model to understand what to use for the force terms in (6) that accounts for this issue.

In Bouzat (2016), the authors make the observation that including cargo noise produces this described difficulty: motors should not react instantaneously to velocity and classical models produce results inconsistent with experimental observations if this is the case. To overcome this issue, the authors hypothesize that the motors respond to a time-windowed-average force, suggesting some "memory" property of the motors. Here, we directly compute a physiological, mechanistic delay stemming from the stepping of the motor, instead of a phenomenological "memory."

2.3.1. Ornstein–Uhlenbeck motivation

To understand motor response to fluctuations in the cargo velocity, we now turn our attention the behavior of an ensemble of M motors on a *single run*: after binding and before unbinding. This focus stems from the observation that force generation can only occur while the motors are bound. The dynamics of force generation are of interest as these dictate the cargo behavior. In McKinley et al. (2012), the authors also study the behavior of motors without binding dynamics and find that multiple motors can actually produce a lower cargo velocity than a single motor. However, in our model, we reiterate that the motors act identically and independently aside from interaction with the cargo, which is addressed separately. Hence, it is sufficient to describe the behavior of a single motor. Let $p_1(x, t)$ describe the probability density of finding a motor stretched distance x from its unstretched position at time t and let $x_1(t)$ be the corresponding Langevin random process.

The behavior follows almost identically with the mean-field model (1), but now binding and unbinding can be neglected due to the analysis only being of a single run. The only remaining dynamics are the motor stepping (still at its force dependent velocity w) and diffusion (the magnitude of which is lumped into a parameter D). The resulting process is an Ornstein–Uhlenbeck process Gardiner (2009), which can be described by the Langevin equation

$$\dot{x}_1 = [w(x_1) - v(t)] + \sqrt{2D}\,\xi(t),$$

or the corresponding Fokker–Planck equation

$$\frac{\partial p_1}{\partial t} = -\frac{\partial}{\partial x}\{[w(x) - v(t)]p_1\} + D\frac{\partial^2 p_1}{\partial x^2}. \tag{7}$$

To quantify the motor's ability to respond to instantaneous fluctuations in the cargo velocity, we consider the mean position of a motor while still attached, denoted μ_1,

$$\mu_1 := \langle x_1(t)\rangle.$$

From the Fokker–Planck equation (7), we find the relationship describing the temporal evolution of the mean of this process to be (assuming w is a linear function)

$$\dot{\mu}_1 = w(\mu_1) - v(t). \tag{8}$$

For details of the calculation, see Appendix A.

However, again recalling the assumption of a Hookean force (that is, force from a single motor stretched distance x_1 is kx_1), the average force exerted by a single motor under evolving under this process with density $p(x_1, t)$ is then

$$F_1 = k\int_{-\infty}^{\infty} x_1 p(x_1,t)\,dx_1 = k\mu_1.$$

and, since we have M motors in our ensemble, the total average force is immediate from linearity

$$F_{tot} = Mk\mu_1. \tag{9}$$

In other words, *for a bound ensemble of motors*, the mean force exerted can be parameterized by the mean distance stretched μ, where μ "tracks" the velocity through (8). This illustrates that the magnitude of the delay in motor response to fluctuations in cargo velocity is determined by the motor velocity. In other words, changes in force are only due to changes in displacement, not

velocity. This resolves the aforementioned issue about the force changing instantaneously. Now, the mean force tracks, with some delay as determined by (8), the velocity and evolves continuously.

2.3.2. Force evolution approximation

The previous calculation showed that while still attached, the mean force generation for a population of motors could be collapsed down to a single parameter μ_1. However, relating the mean-field model to this single-run analysis presents an obvious issue: how to account for binding dynamics? We now make the major approximation of the paper: even with binding and unbinding, the mean force generated by each population of motors can be collapsed to a single parameter μ (for each population) with a similarly structured delay. This leads us to the set of equations (with one motor family for illustration)

$$\mathcal{M}\dot{v} + \gamma v = \hat{F}(\mu) + \sqrt{2\gamma k_B T}\xi(t), \qquad \dot{\mu} = w(\mu) - v. \tag{10}$$

We assume the cargo velocity v fluctuates with the forces exerted on it, but the force exerted by the motors is not directly prescribed by the current v but rather some parameter μ which tracks v with a delay. We note that, in the previous section, we have proven that this delay structure exists while the motors are attached. However, we posit that this delay structure is still appropriate even when binding dynamics are incorporated because force generation on the cargo requires the motors to be attached. In the previous analysis, μ had a physical meaning: the average distance a motor is stretched. However, we lose this meaning and consider μ a "characteristic distance." The force exerted by these motors is also no longer $Mk\mu_1$ because not all motors are bound at any given time, so we give the force a general form $\hat{F}(\mu)$ that is specified later. It is also important to reiterate that (10) is written for a single parameter μ, meaning a single motor population to demonstrate the structure but we later incorporate parameters μ_1, μ_2, one for each population.

The particular choice of the parameterized force $\hat{F}_j(\mu)$ (for $j = 1, 2$, corresponding to each population) must not neglect unbinding and binding of the motors and must account for the fact that not all motors are bound at a given time. We conjecture that a sufficient approximation is the steady-state force $\tilde{F}(\tilde{v})$, originally parameterized by a steady-state cargo velocity $\tilde{v}$, described by (5).

It does not seem immediately clear how to construct a mapping between a value of μ and $\tilde{v}$ to plug into $\tilde{F}$. We recall that $\tilde{F}$ was computed assuming the cargo velocity $\tilde{v}$ was fixed (in steady-state), whereas the true quantity $v(t)$ is constantly fluctuating and never in steady-state. Utilizing the fact that $\tilde{v}$ corresponds to steady-state, we can construct a mapping between μ and $\tilde{v}$ by ensuring that the equilibria of our approximation match the equilibria of the original system. That is, if we are in steady-state, $\dot{\mu} = 0$ and consequently

$$\dot{\mu} = 0 = -a\mu + b - \tilde{v} \quad \Rightarrow \quad \tilde{v} = -a\mu + b.$$

This then provides a mapping between a steady-state cargo velocity $\tilde{v}$ and a particular μ value. Hence, we can now evaluate our force as a function of μ

$$\hat{F}_j(\mu_j) = \tilde{F}_j(-a_j\mu_j + b_j). \tag{11}$$

We reiterate that this approximate system is still inherently out-of-equilibrium, but now, by construction, has equilibria that match the original model since $\dot{\mu} = 0$ corresponds to a particular $\tilde{v}$, a steady-state velocity from which the force was originally computed.

In other words, the motors track the steady state force-velocity curve $\tilde{F}$ with some delay. This particular choice of the force structure allows for the complexity of the mean-field model, including all binding and unbinding to be embedded into the $\tilde{F}(\mu)$ terms. However, the dynamics of the reduced "characteristic distance" model are easier to study due to being an ordinary differential equation rather than a partial differential equation. Our analysis shows that this delay structure is exact for bound motors and this approximation posits an extension of the structure to account for binding and unbinding. We explore the validity of this approximation numerically in Section 3.2.

2.4. Full model

The parameter regime we are considering deals with cargo with negligible mass, thus suggesting we are in a viscous or near-viscous regime. Exploiting this fact, we can perform an adiabatic (quasi-steady state) reduction on (10) to eliminate v. For details of this calculation, see *Supplementary Section S3*. The result of performing this reduction (with a single motor population) is

$$\dot{\mu} = w(\mu) - \frac{\hat{F}(\mu)}{\gamma} + \sqrt{\frac{2k_BT}{\gamma}}\xi(t), \tag{12}$$

or equivalently, in Fokker–Planck form

$$\frac{\partial p}{\partial t} = -\frac{\partial}{\partial \mu}\left\{w(\mu) - \frac{1}{\gamma}\hat{F}(\mu)\right\} + \frac{k_BT}{\gamma}\frac{\partial^2 p}{\partial \mu^2}. \tag{13}$$

One important note from the calculation detailed in *Supplementary Section S3* is that although v is eliminated from the system, v relaxes quickly to a Gaussian centered around

$$\hat{v} \sim \hat{F}(\mu)/\gamma, \tag{14}$$

thus the value of μ directly determines the (mean) velocity of the cargo at any time.

Combining all of the previous observations, we now propose the full model. In the derivation of (12,13), only one motor population was considered, but in bidirectional transport, there are two populations evolving separately, resulting in two equations with identical structure but different parameters. From this, we get the full model

$$\begin{aligned}\dot{\mu}_1 &= -a_1\mu_1 + b_1 - \frac{1}{\gamma}\{F_1(\mu_1) + F_2(\mu_2)\} + \sqrt{\frac{2k_BT}{\gamma}}\xi(t),\\ \dot{\mu}_2 &= -a_2\mu_2 + b_2 - \frac{1}{\gamma}\{F_1(\mu_1) + F_2(\mu_2)\} + \sqrt{\frac{2k_BT}{\gamma}}\xi(t).\end{aligned} \tag{15}$$

Note that we have switched the two populations to labels $j = 1, 2$ instead of $+/-$ and dropped the hat notation from $\hat{F}_j$ for notational convenience. Because the motor populations were originally coupled through the forces, the force terms in (12,13) must be replaced with the sum of forces from each family, and consequently, the Eqs. (15) are coupled. We have also used the functional form of the motor force velocity curve $w(x) = -ax + b$ and that the net force exerted by the motors is simply the sum of the force exerted by each population.

To emphasize the ability of this model to produce bidirectional motion without asymmetry between the motor populations, we take the parameters describing each of the populations to be the same (unless noted otherwise), described in Table 1. These parameters are chosen as physiologically reasonable parameters in the range of reported values of both kinesin and dynein, taken from Kunwar et al. (2008),Schnitzer et al. (2000) and Klumpp et al. (2015). The viscosity of cytoplasm is reported to be higher than water (Luby-Phelps, 2000; Mitchell and Lee, 2009). Although a potentially large viscosity is used in this work, any smaller would only make the magnitude of the fluctuations larger, further magnifying the importance of cargo diffusion.

2.5. Dimensional reduction

An important observation must be made about the noise structure of (15): the white noise term in each equation is exactly the

Table 1
"Typical" motor values used for both populations of motors in the symmetric case of the mean field model. Values used are within reported ranges of kinesin and dynein.

F_{stall} [pN]	v_0 $[\mathrm{nm \cdot s^{-1}}]$	k_{off} $[\mathrm{s^{-1}}]$	$\lvert F_d \rvert$ [pN]	k_{on} $[\mathrm{s^{-1}}]$	M	k $[\mathrm{pN \cdot nm^{-1}}]$	γ $[\mathrm{pN \cdot s \cdot nm^{-1}}]$
5	1000	1	1	5	10	0.4	0.001

same (fully correlated). From a biophysical perspective, this is because the two motors feel the same fluctuations from the cargo diffusion. Hence, this is truly a one-dimensional diffusion rather than two dimensional as it currently appears. The Fokker–Planck equation corresponding to the system (15) has a non-invertible diffusion tensor, which further illustrates this point. To make the one-dimensional structure more apparent, we perform a change of variables, taking

$$\zeta := \mu_1 + \mu_2, \quad \eta := \mu_1 - \mu_2$$

Under this coordinate change, the system (15) becomes, abbreviating $D := k_B T/\gamma$

$$\dot{\zeta} = -\frac{a_1}{2}(\zeta + \eta) + b_1 - \frac{a_2}{2}(\zeta - \eta) + b_2 - \frac{2}{\gamma}\sum_j F_j + 2\sqrt{2D}\xi(t)$$

$$\dot{\eta} = -\frac{a_1}{2}(\zeta + \eta) + b_1 + \frac{a_2}{2}(\zeta - \eta) - b_2.$$

By taking the two populations to be symmetric, which corresponds to $a_1 = a_2 = a$ and $b_1 = -b_2 = b$, the η equation becomes

$$\dot{\eta} = -a\eta + 2b,$$

which has an invariant manifold described by $\tilde{\eta} = 2b/a$. Since the equilibria of the system must lie on this invariant manifold, all dynamics of interest evolve on the manifold and consequently reduces the problem to the one-dimensional evolution

$$\dot{\zeta} = -a\zeta - \frac{2}{\gamma}\left[F_1\left(\frac{\zeta + \tilde{\eta}}{2}\right) + F_2\left(\frac{\zeta - \tilde{\eta}}{2}\right)\right] + 2\sqrt{2D}\xi(t), \qquad (16)$$

where again, $\tilde{\eta} = 2b/a$.

Thus, we have fully reduced the dynamics of the system to a single time-varying quantity ζ, which again does not seem to have a physical meaning but can be thought of as the *characteristic distance* of the system. Although a considerable number of reductions have been made, the physical behavior of the system is still recoverable by recalling that the instantaneous mean cargo velocity, $\hat{v}$, of the system can be recovered from (14). In other words, $\zeta(t)$ is a proxy for $\hat{v}(t)$ which is the biophysical quantity of interest. It is worth noting that the analysis exploits the existence of an invariant manifold, but it does not seem to be the case that such a manifold exists if the populations are asymmetric. Hence, the asymmetric population problem is considerably more difficult to study (as only Monte Carlo simulations seem to be feasible) and not within the scope of this work.

3. Results

3.1. Linear motor force–velocity curve

We briefly explore the consequences of approximating the motor force-velocity curve $w(x)$ as a linear function described in (2). Recall that $w(x)$ is really a *displacement*-velocity curve but force generation is assumed to be Hookean, so the qualitative shape remains the same as the force-velocity curve. We reiterate that a sigmoidal force-velocity relationship seems to be in closer agreement to experimentally observed measurements and used it on other models. However, we posit that the motors operate primarily in a region of the force-velocity curve that can be approximated by its linearization. To assess the validity of this approximation, we relaxed the assumption of linearity on $w(x)$ and changed the functional form to be of the form $\bar{w}(x) = \alpha_0 + \alpha_1 \tanh(\alpha_2(x - \alpha_3))$, a particular sigmoidal function utilized in previous work (McKinley et al., 2012). We then compare the steady-state ensemble force-velocity described by (5) produced by the linear $w(x)$ and two different parameter choices of the sigmoidal form that vary only by how quickly they saturate. The result of this comparison can be seen in Fig. 2. From this figure, we can see that the force-velocity curves produced for the ensemble (on the right) vary very little when the form of $w(x)$ is changed. There is excellent qualitative agreement and even good quantitative agreement, seeming to only differ for sufficiently large velocities outside the scope of the model. Thus, we conclude the use of the linearized $w(x)$ is suitable for the analysis, particularly noting that $\tilde{F}$ is the effectively only quantity used from the mean-field model and remains virtually the same. We conjecture this result can be interpreted intuitively, as superstall velocities are larger in magnitude by our approximation, meaning that the motors relax back to stall faster and therefore generate a smaller force due to displacement. This is offset by the motors unbinding less rapidly (due to a lower force), and consequently the net force generated is approximately the same.

3.2. Force delay approximation

The form of the system (10) is an approximation which describes a delay structure, where the force generated by a family of motors can be parameterized by a single dynamic quantity, μ. We prove this to be the case while the motors are bound with (9) and (12), but the heart of the approximation is that this extends to when binding dynamics are incorporated. We posit that a sufficient approximation to the instantaneous force generated is the steady-state ensemble force $\tilde{F}(\tilde{v})$ with a particular mapping between μ and $\tilde{v}$ described by (11). We seek to assess the validity of the collapse of the force generated by the mean-field equation to a force parameterized by μ. Specifically, we compare numerical simulations of the full mean-field model (1,3) and the reduced model (10). This numerical simulation is *not* an assessment of the validity of the mean-field model, but rather the validity of the force generated by collapsing the PDE behavior down to a single ODE for μ.

We simulate only a single motor family (+ direction) and no thermal noise for illustration. The approximation fundamentally is one of how motors (and the force generated by them) respond temporally, so a numerical experiment is performed by applying instantaneous external forces to both the mean field model of motors and the reduced model, both of which have cargo dynamics determined by (6). Both models are started at the completely unloaded state and run to equilibrium. Once at equilibrium, a -5 pN force (and later +5 pN) external force is applied to the cargo for 5 ms and then removed. The mean-field PDE was simulated using a Lax–Wendroff scheme and the remaining ODEs are computed using a Runge–Kutta 4(5) scheme. The dynamics of the force generated by the motor population and the resulting cargo velocity are tracked and shown in Fig. 3.

From Fig. 3 we are able to make a number of observations about the validity of the "characteristic distance" approximation. For one, the equilibria of the full model and reduced model are the same, which is immediate by the choice of (11), but also indicates

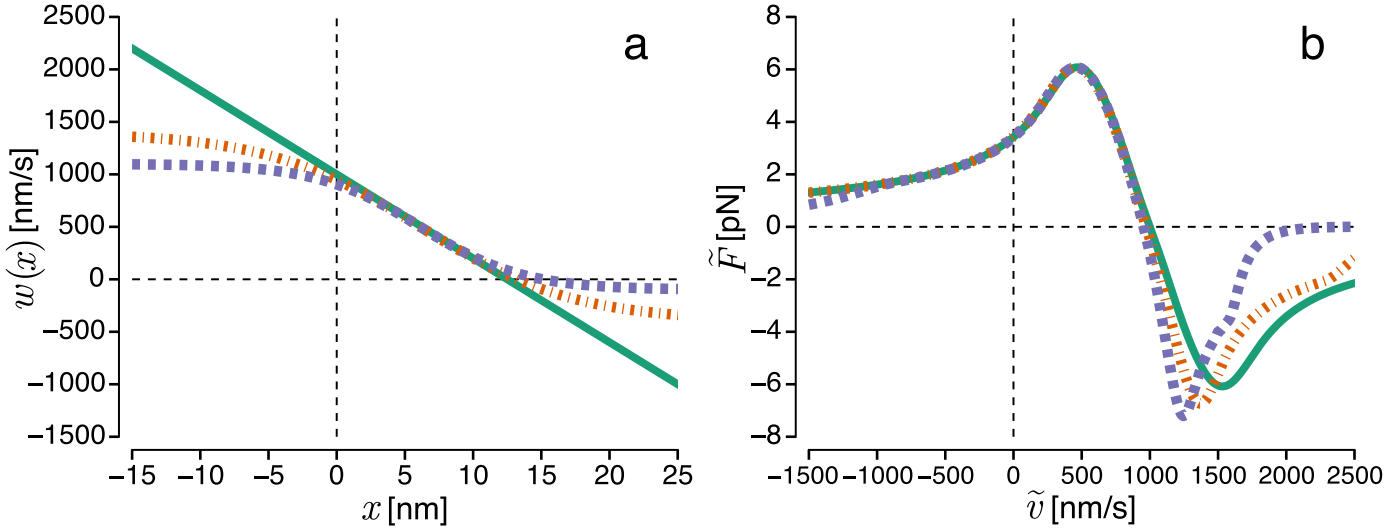

Fig. 2. **a:** the linear form (green, solid) of the displacement-velocity relationship of individual motors $w(x)$ used throughout the paper and two different sigmoidal versions for comparison (dotted). **b:** the resulting steady-state force-velocity curves for the ensemble of motors described by (5) for the different choices of $w(x)$. (For interpretation of the references to colour in this figure legend, the reader is referred to the web version of this article.)

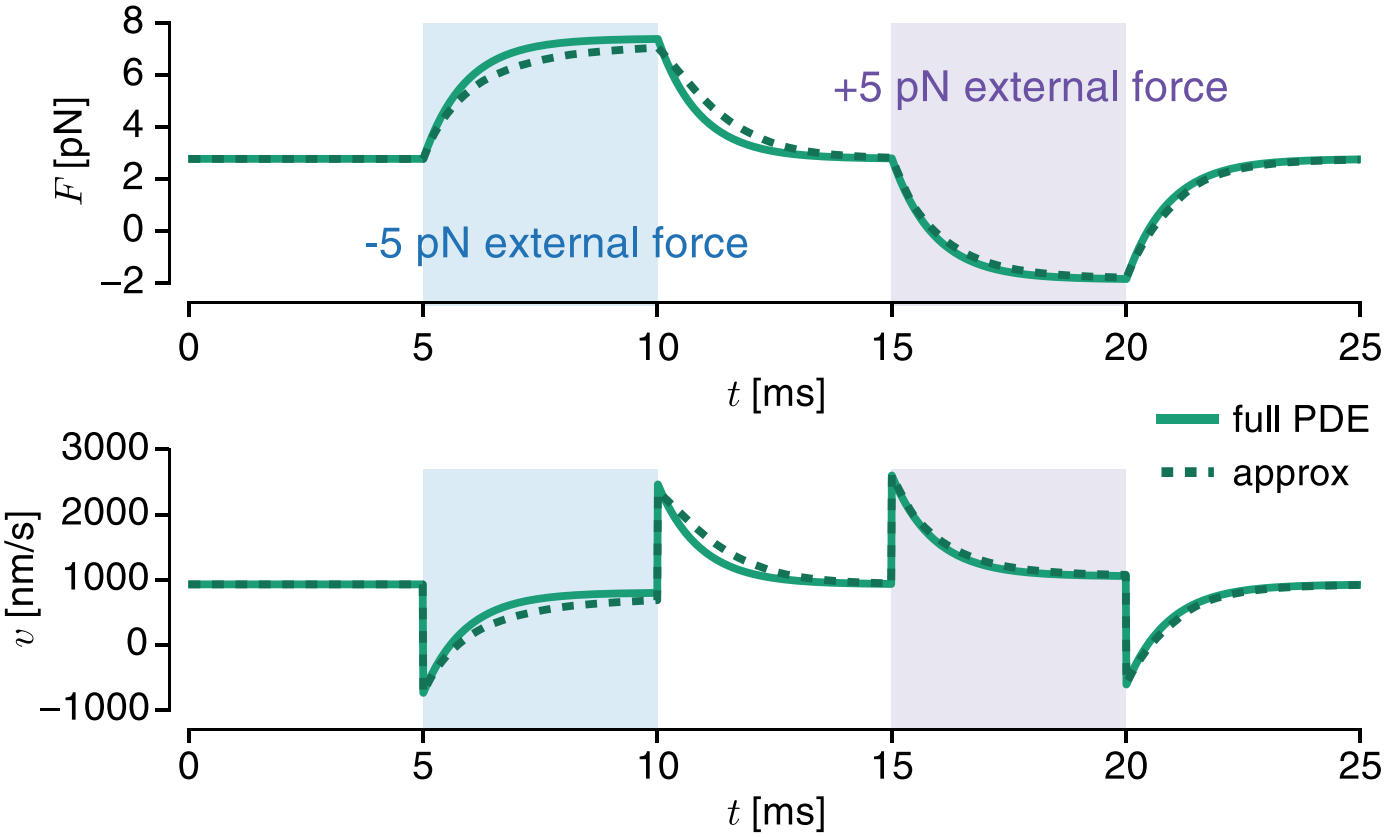

Fig. 3. A numerical comparison of the forces and cargo velocity generated by the full mean field motor model (1,3) with the "characteristic distance" approximation described by (10) for one motor population and no thermal noise. In both models, the evolution of the cargo velocity is described by (6). External forces are applied to the cargo and removed to illustrate the ability of the reduced model to respond to temporal changes in force.

that the reduced and full models have agreement on long time scales. As the external force changes instantaneously, both models behave (quantitatively and qualitatively) similarly regardless of the directionality of the force, and therefore, suggests there is also agreement on short time scales. Other external inputs (e.g. sinusoid) were also investigated and yielded similar results. Thus, we have collapsed the force generated by the PDE mean-field description of motors (1,3) into an ODE (10) in a "characteristic distance" variable and the approximation appears to be valid. We remind the reader that the binding dynamics are built into the mean-field structure, and therefore are accounted for in both the full model and reduced.

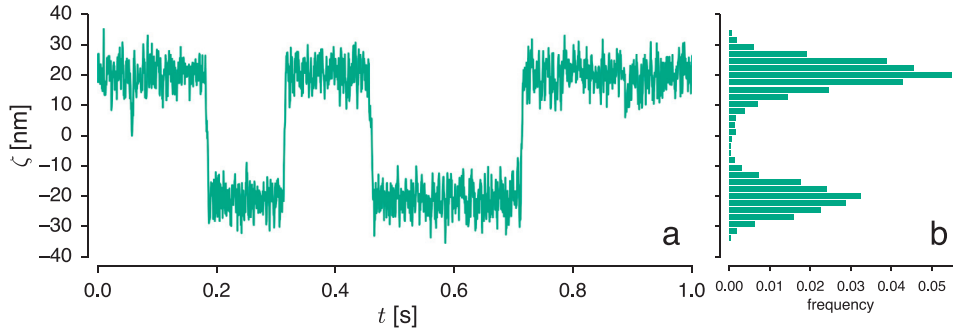

Fig. 4. a: A typical simulation of (16) performed with the Euler–Maruyama scheme. The system notably switches between two configurations. **b:** A histogram of the values of the simulation, which demonstrates bimodality.

3.3. Metastable behavior

We perform simulations of (16) with the parameters specified in Table 1 with the Euler–Maruyama scheme (Kloeden and Platen, 1992). The results of a typical simulation can be seen in Fig. 4a. From this simulation, we see a curious behavior: the characteristic distance ζ switches between two configurations, or is said to be *metastable*. Elaborating on this, ζ takes on values near some particular point and then, due to the noise of the system, randomly switches to values centered around another point. The histogram of ζ values during the simulation, which can also be seen in Fig. 4b is clearly bimodal, which is a characteristic sign of metastability. Although the two peaks in the figure appear different, this is a consequence of the short time for which the simulation was performed. If more switches were recorded, the two peaks of the histogram would be identical due to the symmetric population assumption, however this time frame was chosen to demonstrate the time-scale on which switching occurs.

The metastable behavior of the system is apparent from simulations, but can be further elucidated. To do so, consider the corresponding Fokker–Planck equation to (16), which describes the probability density $p(\zeta, t|\zeta_0, 0)$. That is, the probability density of (16) given that it started at ζ_0, which is described by

$$\partial_t p = -\partial_\zeta \{A(\zeta)p\} + 4D\partial_{\zeta\zeta} p, \tag{17}$$

where we are abbreviating

$$A(\zeta) := -a\zeta - \frac{2}{\gamma}\left[F_1\left(\frac{\zeta+\tilde{\eta}}{2}\right) + F_2\left(\frac{\zeta-\tilde{\eta}}{2}\right)\right], \qquad D := \frac{k_B T}{\gamma}. \tag{18}$$

A bifurcation diagram of the equilibria of $A(\zeta)$ is constructed by varying γ, the drag coefficient. Since ζ is not the physical quantity of interest, we translate the equilibria of ζ into the corresponding mean cargo velocity $\tilde{v}$ under the transformation described by (14). The resulting bifurcation diagram can be seen in Fig. 5a. This figure captures exactly the phenomenon described as *bidirectional motion* (Hancock, 2014). We see that for a robust range of γ, the system is *bistable*: there are stable positive and negative mean cargo velocities, which we will denote v_+, v_- respectively. In this same regime, the zero velocity v_0 is unstable. Interestingly, in small window of γ values, the system is actually *tristable*: two new equilibria emerge in a bifurcation and cause v_0 to turn stable. This may correspond to the experimental observation (Kunwar et al., 2011) that the system can spend long periods of time in a "pause" state, also noting that this same experimental work suggests velocities that agree with those predicted by our model. For large values of γ, the system only has one stable equilibrium, v_0.

From, Fig. 5a, the tristable region in γ-space is fairly narrow. It is possible that other parameters (or more detailed functional forms) would allow for this region to be more robust, but this is not observed. In fact, increasing motor processivity by lowering the baseline unbinding rate by an order of magnitude ($k_{\text{off}} = 1\,[\text{s}^{-1}] \to 0.1\,[\text{s}^{-1}]$) resulted in a *smaller* region of tristability, but larger region of bistability. For this reason, we instead focus our study toward the bistable region, where we study the time to switch between the positive and negative velocities. Then, the corresponding potential can be defined by

$$U(\zeta) := -\int A(\chi)\,\mathrm{d}\chi. \tag{19}$$

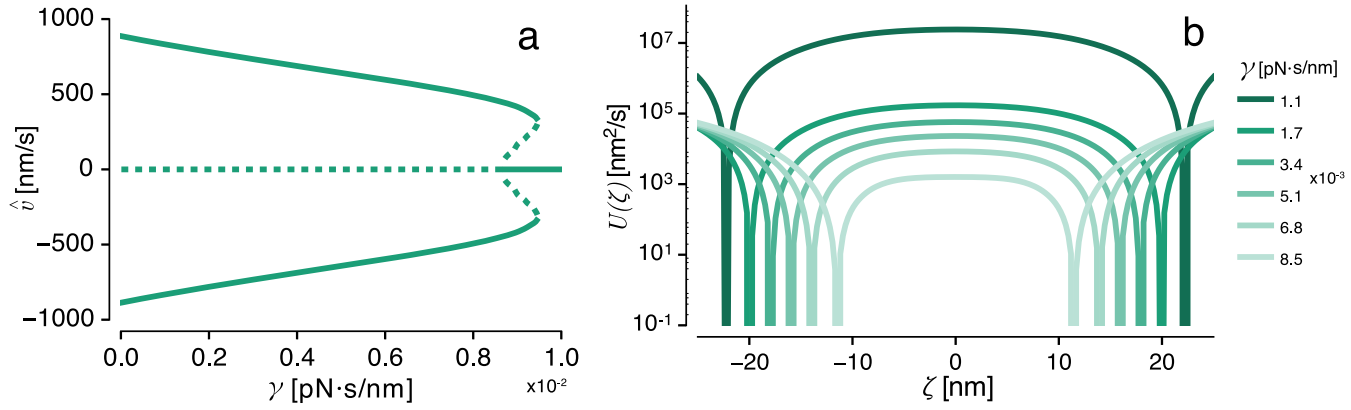

Fig. 5. a: A bifurcation diagram (as a function of the cargo drag, γ) for the system, which is computed from the equilibria of (18) and then translated into mean cargo velocities by (14). Dotted lines correspond to unstable equilibria and solid lines are stable. In a wide range of γ, the system demonstrates a stable positive and negative velocities, or bidirectional motion. **b:** the double-well potential structure (19) as a function of the drag coefficient γ. As γ decreases, the wells get steeper and farther apart.

This potential $U(\zeta)$ can be plotted as a function of γ in the bistable region of Fig. 5a and the result is seen in Fig. 5b. From the figure, we see that $U(\zeta)$ is a double-well potential. That is, there are two distinct well locations and a peak in the center, all three of which are roots of $A(\zeta)$. Denote the two well locations (stable fixed points of $A(\zeta)$) as ζ_{S1} and ζ_{S2}, where $\zeta_{S1} < \zeta_{S2}$ and the middle peak (a hyperbolic fixed point of $A(\zeta)$) as ζ_H.

The effect of the drag coefficient γ on the potential is non-trivial. Particularly, as γ decreases, the wells of the potential $U(\zeta)$ deepen and split farther apart, which alone would suggest an increase in time to switch. However, we later see that there is a counteracting effect in the strength of diffusion.

3.4. Mean first passage time analysis

One natural quantity to study in bidirectional systems is the time to switch directions, or the reversal time. Because of the double-potential well structure, this can be thought of as the mean time from one of the metastable points to the hyperbolic point, from which the system relaxes quickly to the other metastable point. Due to the symmetric motor population assumption, the time to switch states is independent of state. Thus, without loss of generality, we compute the mean first passage time from $\zeta_{S1} \to \zeta_{S2}$ where, again, $\zeta_{S1} < \zeta_H < \zeta_{S2}$.

The analysis of a mean first passage time in a one-dimensional potential is classical (Bressloff, 2014; Gardiner, 2009) and is briefly summarized here. Define $G(z, t)$ to be the probability that the system described by (17) is in the leftmost potential well at time t given the initial state $p(\zeta, 0) = z$. That is, the survival probability density is described by

$$G(z,t) := \int_{\zeta_{S1}}^{\zeta_H} p(\zeta, t \,|\, z, 0)\, \mathrm{d}\zeta.$$

Then, let $T(z)$ define the random variable describing the exit time from this potential well , which satisfies

$$\mathbb{P}[T(z) \le t] = 1 - G(z,t). \tag{20}$$

Taking a derivative of (20) yields the density for exit time $f(z, t)$

$$f(z,t) = -\partial_t G(z,t) = -\int_{\zeta_{S1}}^{\zeta_H} \partial_t p(\zeta, t \,|\, z, 0)\, \mathrm{d}\zeta.$$

From this, we can define the mean first exit time from the potential well, starting at the point z by

$$\tau(z) := \langle T(z) \rangle = \int_0^\infty t f(z,t)\, \mathrm{d}t = \int_0^\infty G(z,t)\, \mathrm{d}t. \tag{21}$$

The survival probability $G(z, t)$ satisfies the backward Fokker–Planck equation (Gardiner, 2009), which we can integrate and use (21) to yield the governing equation for the mean exit time density of the system starting at $\zeta_0 = z$, which is

$$A(z)\tau' + 4D\tau'' = -1, \qquad \tau(\zeta_H) = 0, \qquad \tau'(\zeta_{S1}) = 0. \tag{22}$$

The reflecting boundary at ζ_{S1} is a consequence of starting the system in the well corresponding to this point, as any excursions to the left will quickly relax back to the bottom of the well. The exit location, the hyperbolic point ζ_H, is an absorbing state due to the fast relaxation to the other potential well once the system transverses the peak between them.

The boundary value problem (22) does not appear to be solvable analytically due to the complexity of the force curves. However, $\tau(z)$ can be computed numerically in a straightforward manner (in a single integration) by exploiting the linearity of the system. Alternatively, a deep-well approximation can be made for the potential and the classical *Arrhenius formula* can be used to approximate the mean first passage time. For details on both of these methods, see Appendix B.

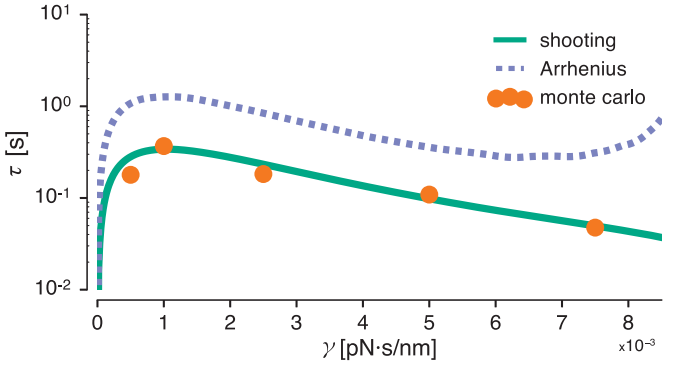

Fig. 6. Mean first passage times corresponding to the cargo switching directions. Two approaches to solving (22) are illustrated: a shooting technique, and the deep-well Arrhenius approximation. The results of an Euler-Maruyama simulation of (16) are also shown, where switching is considered passing through the hyperbolic point.

The two aforementioned techniques of evaluating $\tau(\zeta_{S1})$ are computed and compared against Monte Carlo simulations of (16), again using the Euler-Maruyama scheme, where switching is considered passing the hyperbolic point. The result of these techniques can be seen in Fig. 6. From this, we see that the shooting technique agrees with Monte Carlo simulations and the deep-well approximation is, although qualitatively similar, an overestimate of the switching time. This result is intuitive, as in reality, the wells may not be sufficiently deep for the approximation to work well and therefore allow escape much faster.

The behavior of the mean first passage times as a function of the drag, γ is quite interestingly, non-monotonic. That is, as the drag coefficient increases (which can be thought of as the cargo increasing in size), the time to switch initially goes up, but then ultimately goes back down. Mathematically, this complexity stems from γ scaling both the potential and the diffusion strength differently, explicitly in (18). As γ decreases, the potential wells deepen and spread apart as $\sim 1/\gamma$, but the strength of diffusion simultaneously scales by $\sim \sqrt{1/\gamma}$, which are competing effects for the switching time. The resulting behavior is therefore a complex competition between the scaling of the potential and the noise strength, which produces non-monotonicity. Switching due to motor binding and unbinding is *not* expected to demonstrate this same non-monotonicity, as this is a feature of the mismatched scaling in the strength of the driving noise source (diffusion) and the depth of the potential wells. In other words, γ does not scale the driving noise source the same way for motor binding dynamics. In other theoretical works that compute the switching time, monotonicity is seen (Guérin et al., 2011a; 2011b).

From a biophysical perspective, it should be noted that the predicted mean first passage times are on the order of ~ 0.5[s], which agrees with experimentally observed values (Kunwar et al., 2011). This agreement supports the hypothesis that cargo diffusion is the noise source for bidirectionality. The non-monotonicity of the curve also provides a testable experimental prediction. That is, bidirectional motion via molecular motors could be observed for different cargo drag values (which, could be obtained by varying bead size). If the resulting mean time to switch directions is found to be non-monotonic, this would further strengthen our theory that cargo diffusion, not motor binding dynamics are indeed the noise source of bidirectionality.

4. Discussion & conclusion

In this work, we have proposed a mean-field, unequally distributed load description of motor-mediated transport. To under-

stand the behavior of this complex model, we perform a series of reductions. To justify the first reduction, we take an aside to study only motors that are bound. Of these bound motors, we find that the force generated displays a delay structure that collapses the dimensionality of the system greatly. We posit that, since bound motors are the only contributor to force generation, this delay structure is applicable to the full system even when binding dynamics are incorporated. This allows for the reduction of a PDE describing each motor population to a single ODE for each, describing a "characteristic distance." Secondly, we use the small mass of the cargo to perform an adiabatic (quasi-steady state) reduction of the system. Due to a correlated noise structure and symmetry in the system, the final result is a one-dimensional system, the value of which is a proxy for the instantaneous cargo velocity. This resulting stochastic dynamics are observed to be "metastable", switching between two distinct states exclusively due of cargo diffusion. These states are associated with positive and negative cargo velocities, meaning the system is bidirectional. To quantify the reversal time of the system, a mean-first passage time analysis is performed and the results are explored as a function of the cargo drag, an experimentally tunable quantity. We find that the predicted switching time agrees with experimental values and also has a non-monotonic dependence on cargo drag, a claim that can be experimentally verified.

The use of a mean-field model in this work was not rigorously justified, and could perhaps be made so by starting with a discrete motor model akin to McKinley et al. (2012). Despite this, the mean-field model is able to accurately reproduce experimentally observed ensemble switching times and mean velocities from single-motor parameters. For this reason, we believe the mean-field model to be an appropriate description of the system, but the extent to which it is appropriate could be explored in future work. One notable behavior of our mean-field model is the instability of the pause state for a wide range of parameter values. Intuitively, any small perturbation away from the pause state will produce asymmetry in the system and ultimately result in one motor population "winning." However, it is well established experimentally that bidirectional systems spend a non-trivial amount of time in the paused state (Belyy et al., 2016; Derr et al., 2012), which has also been reproduced in discrete motor simulations such as Müller et al. (2008). This perhaps gives a clue toward when the mean-field model may break down. In the pause state, the motor number may be so low that the mean-field model is not appropriate and consequently, deviates from a discrete motor description. However, we see that in some parameter regimes, the mean-field model is even able to produce a metastable pause state (and consequently, a tristable system). Hence, this conjectured relationship between the use of a mean-field model and the instability of the pause state must be explored further.

The Ornstein-Uhlenbeck analysis for quantifying the ability of a motor to react to instantaneous changes in cargo velocity is of interest in other recent work (Bouzat, 2016) and in general, causes issue in any work that seeks to use a force-velocity relationship (which is inherently a steady-state analysis) to infer dynamics. In Bouzat (2016), the authors hypothesize a "motor memory" and conclude that models only agree with experimental values appropriately if the motors react to a windowed-time-average velocity. By examining only bound motors, we have quantified this "memory" physiologically, noting a distinct delay structure. Because bound motors are the force-generators of the system, we proposed a novel approximation to the full dynamics that satisfies the same delay structure, the validity of which was supported by numerical simulations. A more elegant approach to this approximation may be possible and could perhaps be related to the more detailed analysis of bound motor dynamics found in McKinley et al. (2012).

In Bouzat (2016), the authors also cite the importance of cargo diffusion in models producing results that match experimental values. In our work, we have further illustrated the importance of cargo diffusion by illustrating its ability to produce qualitative changes in motor-mediated transport. Specifically, the fundamental noise driving switching in our model is cargo diffusion, unlike previous unequally distributed load models which depended on a discrete motor description. This raises the possibility of the importance of diffusion in other aspects of motor-mediated transport.

Thus, we have illustrated that common features of previous work: discreteness of the motors, asymmetry of motor populations, equally distributed loads are *not* necessary to produce a physiologically reasonable model of bidirectional motor transport. This raises uncertainty of which key ingredients may be essential for tug-of-war, making it even more difficult to compare to the alternative regulatory hypothesis of bidirectionality. However, we have provided an experimentally testable prediction of the reversal time as a function of the drag coefficient, which can be tuned by the bead size in experimental setups. If indeed thermal noise is the driver of this switching, then agreement with this experiment would help strengthen the validity of this theory since this feature is not expected from motor binding dynamics as the driving noise source.

Acknowledgments

This research was partially supported by NSF grant DMS 1122297 and DMS-RTG 1148230.

Appendix A. Ornstein–Uhlenbeck Mean Evolution

In this section, we show that if the advection term of an Ornstein–Uhlenbeck has a time dependence, a differential equation can be obtained for the mean of the process, demonstrating an effective delay.

Consider a Fokker–Planck equation of the form

$$\partial_t p = -\partial_x[\{w(x) - v(t)\}p] + D\partial_{xx}p. \tag{A.1}$$

Denote $\mu(t)$ to be the mean of the process, that is $\mu = \langle p \rangle$. Then, we have:

$$\dot{\mu} = \frac{\mathrm{d}}{\mathrm{d}t}\int_{-\infty}^{\infty} x\, p(x,t)\,\mathrm{d}x = \int_{-\infty}^{\infty} x\partial_t p\,\mathrm{d}x.$$

However, we can use (A.1) to find that

$$\dot{\mu} = -\int_{-\infty}^{\infty} x\partial_x[\{w(x) - v(t)\}p]\,\mathrm{d}x + \int_{-\infty}^{\infty} xD\partial_{xx}p\,\mathrm{d}x,$$

which, after integration by parts, yields

$$\dot{\mu} = \langle w(x)\rangle - v.$$

Jensen's inequality states that for a convex w

$$\langle w(x)\rangle \geq w(\langle x\rangle),$$

however, if we assume $w(x)$ is *linear* (as we have done in the model), then Jensen's inequality attains equality and the result is

$$\dot{\mu} = w(\mu) - v(t).$$

Appendix B. Methods for 1D MFPT Problems

For the sake of generality, consider the one dimensional SDE

$$\mathrm{d}x = A(x)\mathrm{d}t + \sqrt{2B(x)}\,\mathrm{d}W,$$

which has a corresponding Fokker–Planck equation

$$\partial_t p = -\partial_x\{A(x)p\} + B(x)\partial_{xx}p.$$

We are assuming that $A(x)$ has three fixed points, two stable and one hyperbolic, denote x_S and x_H.

We are then interested in the mean first passage time starting from a point y, which we denote $\tau(y)$, and satisfies

$$A(y)\tau' + B(y)\tau'' = -1, \qquad \tau'(x_S) = 0, \qquad \tau(x_H) = 0. \tag{B.1}$$

B1. Shooting method

In this section, we exploit the linearity of (B.1) to construct a numerical shooting method for constructing a solution. First, we write the system as a first order system, by taking $\sigma = \tau'$,

$$\begin{bmatrix}\tau'\\ \sigma'\end{bmatrix} + \begin{bmatrix}0 & 1\\ 0 & \frac{A(x)}{B(x)}\end{bmatrix}\begin{bmatrix}\tau\\ \sigma\end{bmatrix} = \begin{bmatrix}0\\ -\frac{1}{B(x)}\end{bmatrix}, \qquad \begin{bmatrix}\tau(x_H)\\ \sigma(x_S)\end{bmatrix} = \begin{bmatrix}0\\ 0\end{bmatrix}. \tag{B.2}$$

To construct a solution to (B.2), we obtain two solutions of initial value problems of the same form and utilize the linearity of the equation to solve the boundary value problem via superposition. Thus, consider the following two systems:

$$\begin{bmatrix}p_1'\\ p_2'\end{bmatrix} + \begin{bmatrix}0 & 1\\ 0 & \frac{A(x)}{B(x)}\end{bmatrix}\begin{bmatrix}p_1\\ p_2\end{bmatrix} = \begin{bmatrix}0\\ -\frac{1}{B(x)}\end{bmatrix}, \qquad \begin{bmatrix}p_1(x_S)\\ p_2(x_S)\end{bmatrix} = \begin{bmatrix}0\\ 0\end{bmatrix}$$

$$\begin{bmatrix}q_1'\\ q_2'\end{bmatrix} + \begin{bmatrix}0 & 1\\ 0 & \frac{A(x)}{B(x)}\end{bmatrix}\begin{bmatrix}q_1\\ q_2\end{bmatrix} = \begin{bmatrix}0\\ 0\end{bmatrix}, \qquad \begin{bmatrix}q_1(x_S)\\ q_2(x_S)\end{bmatrix} = \begin{bmatrix}1\\ 0\end{bmatrix}$$

We now claim $\Upsilon = \begin{bmatrix}\tau & \sigma\end{bmatrix}^T$ is a linear combination of $P = \begin{bmatrix}p_1 & p_2\end{bmatrix}^T$ and $Q = \begin{bmatrix}q_1 & q_2\end{bmatrix}^T$. In other words, there exists some γ such that $\Upsilon = P + \gamma Q$. The value of γ is to be determined by making sure the right boundary condition is satisfied

$$\tau(x_H) = p_1(x_H) + \gamma q_1(x_H) = 0 \Rightarrow \gamma = -\frac{p_1(x_H)}{q_1(x_H)}.$$

Thus, our mean first passage time from $x_S \to x_H$ is then

$$\tau(x_S) = p_1(x_S) + \gamma q_1(x_S) = \gamma.$$

It is worth noting that this actually only requires a *single* ODE integration, as Q is identically constant by construction with $q_1 \equiv 1$ and $q_2 \equiv 0$, and consequently

$$\gamma = -p_1(x_H).$$

B2. Arrhenius (deep well) approximation

The deep-well approximation is a classical technique used to compute the mean first passage time from a potential well. Here, we briefly summarize the technique but additional details can be found in Gardiner (2009) and Bressloff (2014). Following the latter reference, define the potential function $U'(y) := -A(y)$, so $U = -\int A(y)\,dy$. After using an integrating factor and assuming B is constant for simplicity, we have

$$\tau = \frac{1}{B}\int_{x_S}^{x} e^{U(x')/B}\,dx' \int_0^{x'} e^{-U''(x'')/B}\,dx'',$$

noting that we have also taken $0 < x_S < x_H$ for convenience. Assuming the potential is deep-welled, the first integral is sharply peaked around $x' = x_H$, where the second integral is slowly varying. For this reason, we can interchange the limits of the integral to obtain

$$\tau = \frac{1}{B}\left[\int_0^{x_H} e^{-U(x'')/B}\,dx''\right]\left[\int_{x_S}^{x} e^{U(x')/B}\,dx'\right].$$

Now, the first integral is dominated around $x'' = x_H$, whereas the second is dominated around $x' = x_S$ so that the limits can be taken to infinity with little error. Using the method of steepest descent (or simply, a Taylor expansion), we finally have the classical *Arrhenius formula*

$$\tau \sim \frac{2\pi}{\sqrt{|U''(x_H)|U''(x_S)}} e^{(\Delta U)/B}, \qquad \Delta U := U(x_H) - U(x_S).$$

Supplementary material

Supplementary material associated with this article can be found, in the online version, at 10.1016/j.jtbi.2017.04.032.

References

Andreasson, J.O., Milic, B., Chen, G.-Y., Guydosh, N.R., Hancock, W.O., Block, S.M., 2015. Examining kinesin processivity within a general gating framework. Elife 4, e07403. doi:10.7554/eLife.07403.

Belyy, V., Hendel, N.L., Chien, A., Yildiz, A., 2014. Cytoplasmic dynein transports cargos via load-sharing between the heads. Nat. Commun. 5, 5544. doi:10.1038/ncomms6544.

Belyy, V., Schlager, M.A., Foster, H., Reimer, A.E., Carter, A.P., Yildiz, A., 2016. The mammalian dyneindynactin complex is a strong opponent to kinesin in a tug-of-war competition. Nat. Cell Biol. 18 (9), 1018–1024. doi:10.1038/ncb3393.

Bouzat, S., 2016. Models for microtubule cargo transport coupling the langevin equation to stochastic stepping motor dynamics: caring about fluctuations. Phys. Rev. E 93 (1), 012401. doi:10.1103/PhysRevE.93.012401.

Bressloff, P.C., 2014. Stochastic Processes in Cell Biology. Interdisciplinary Applied Mathematics, 41. Springer International Publishing doi:10.1007/978-3-319-08488-6.

Bressloff, P.C., Levien, E., 2015. Synaptic democracy and vesicular transport in axons. Phys. Rev. Lett. 114 (16), 1–5. doi:10.1103/PhysRevLett.114.168101.

Brooks, H.A., Bressloff, P.C., 2016. A mechanism for turing pattern formation with active and passive transport. SIAM J. Appl. Dyn. Syst. 15 (4), 1823–1843. doi:10.1137/16M1061205.

Carter, N.J., Cross, R.A., 2005. Mechanics of the kinesin step. Nature 435 (7040), 308–312. doi:10.1038/nature03528.

Derr, N.D., Goodman, B.S., Jungmann, R., Leschziner, A.E., Shih, W.M., Reck-Peterson, S.L., 2012. Tug-of-War in motor protein ensembles. Science 338, 662–666. doi:10.1126/science.1226734.

Fu, M.-M., Holzbaur, E.L.F., 2014. Integrated regulation of motor-driven organelle transport by scaffolding proteins. Trends Cell Biol. 24 (10), 564–574. doi:10.1016/j.tcb.2014.05.002.

Gardiner, C., 2009. Stochastic Methods: A Handbook for the Natural and Social Sciences. Springer Series in Synergetics, 13, 4th Springer Berlin Heidelberg doi:10.1007/978-3-662-02377-8.

Gennerich, A., Carter, A.P., Reck-Peterson, S.L., Vale, R.D., 2007. Force-Induced bidirectional stepping of cytoplasmic dynein. Cell 131 (5), 952–965. doi:10.1016/j.cell.2007.10.016.

Gross, S.P., Vershinin, M., Shubeita, G.T., 2007. Cargo transport: two motors are sometimes better than one. Curr. Biol. 17 (12), R478–R486. doi:10.1016/j.cub.2007.04.025.

Guérin, T., Prost, J., Joanny, J.-F., 2011a. Bidirectional motion of motor assemblies and the weak-noise escape problem. Phys. Rev. E 84 (4), 041901. doi:10.1103/PhysRevE.84.041901.

Guérin, T., Prost, J., Joanny, J.-F., 2011b. Motion reversal of molecular motor assemblies due to weak noise. Phys. Rev. Lett. 106 (6), 068101. doi:10.1103/PhysRevLett.106.068101.

Hancock, W.O., 2014. Bidirectional cargo transport: moving beyond tug of war. Nat. Rev. Mol. Cell Biol. 15 (9), 615–628. doi:10.1038/nrm3853.

Hendricks, A.G., Perlson, E., Ross, J.L., Schroeder, H.W., Tokito, M., Holzbaur, E.L.F., 2010. Motor coordination via a tug-of-War mechanism drives bidirectional vesicle transport. Curr. Biol. 20 (8), 697–702. doi:10.1016/j.cub.2010.02.058.

Howard, J., 2001. Mechanics of Motor Proteins and the Cytoskeleton. Sinauer Associates.

Huxley, A.F., 1957. Muscle structure and theories of contraction. Prog. Biophys. Biophys. Chem. 7, 255–318.

Kawaguchi, K., Uemura, S., Ishiwata, S., 2003. Equilibrium and transition between single- and double-Headed binding of kinesin as revealed by single-Molecule mechanics. Biophys. J. 84 (2), 1103–1113. doi:10.1016/S0006-3495(03)74926-1.

Keener, J.P., Sneyd, J., 2008. Mathematical Physiology. Springer Science & Business Media doi:10.1007/978-0-387-79388-7.

Kloeden, P.E., Platen, E., 1992. Numerical Solution of Stochastic Differential Equations. Stochastic Modelling and Applied Probability, 23. Springer doi:10.1080/17442509408833885.

Klumpp, S., Berger, F., Lipowsky, R., 2015. Molecular motors: cooperative phenomena of multiple molecularmotors. In: De, S., Hwang, W., Kuhl, E. (Eds.), Multiscale Model. Biomech. Mechanobiol. chapter 3. Springer London, London, p. 287. doi:10.1007/978-1-4471-6599-6.

Kunwar, A., Tripathy, S.K., Xu, J., Mattson, M.K., Anand, P., Sigua, R., Vershinin, M., McKenney, R.J., Yu, C.C., Mogilner, A., Gross, S.P., 2011. Mechanical stochastic tug-of-war models cannot explain bidirectional lipid-droplet transport. Proc. Natl. Acad. Sci. 108 (47), 18960–18965. doi:10.1073/pnas.1107841108.

Kunwar, A., Vershinin, M., Xu, J., Gross, S.P., 2008. Stepping, strain gating, and an unexpected force-Velocity curve for multiple-Motor-Based transport. Curr. Biol. 18 (16), 1173–1183. doi:10.1016/j.cub.2008.07.027.

Lindemann, C.B., Hunt, A.J., 2003. Does axonemal dynein push, pull, or oscillate? Cell Motil. Cytoskeleton 56 (4), 237–244. doi:10.1002/cm.10148.

Lipowsky, R., Beeg, J., Dimova, R., Klumpp, S., Müller, M.J., 2010. Cooperative behavior of molecular motors: cargo transport and traffic phenomena. Physica E 42 (3), 649–661. doi:10.1016/j.physe.2009.08.010.

Lipowsky, R., Chai, Y., Klumpp, S., Liepelt, S., Müller, M.J., 2006. Molecular motor traffic: from biological nanomachines to macroscopic transport. Physica A 372 (1), 34–51. doi:10.1016/j.physa.2006.05.019.

Luby-Phelps, K., 2000. Cytoarchitecture and physical properties of cytoplasm: volume, viscosity, diffusion, intracellular surface area. Int. Rev. Cytol. 192, 189–221.

McKenney, R.J., Vershinin, M., Kunwar, A., Value, R.B., Gross, S.P., 2010. LIS1 And nude induce a persistent dynein force-Producing state. Cell 141 (2), 304–314. doi:10.1016/j.cell.2010.02.035.

McKinley, S.A., Athreya, A., Fricks, J., Kramer, P.R., 2012. Asymptotic analysis of microtubule-based transport by multiple identical molecular motors. J. Theor. Biol. 305, 54–69. doi:10.1016/j.jtbi.2012.03.035.

Mitchell, C.S., Lee, R.H., 2009. A quantitative examination of the role of cargo-exerted forces in axonal transport. J. Theor. Biol. 257 (3), 430–437. doi:10.1016/j.jtbi.2008.12.011.

Müller, M.J., Klumpp, S., Lipowsky, R., 2008. Tug-of-war as a cooperative mechanism for bidirectional cargo transport by molecular motors. Proc. Natl. Acad. Sci. 105 (12), 4609–4614. doi:10.1073/pnas.0706825105.

Nadrowski, B., Martin, P., Julicher, F., 2004. Active hair-bundle motility harnesses noise to operate near an optimum of mechanosensitivity. Proc. Natl. Acad. Sci. 101 (33), 12195–12200. doi:10.1073/pnas.0403020101.

Nicholas, M.P., Höök, P., Brenner, S., Wynne, C.L., Vallee, R.B., Gennerich, A., 2015. Control of cytoplasmic dynein force production and processivity by its c-terminal domain. Nat. Commun. 6, 6206. doi:10.1038/ncomms7206.

Osunbayo, O., Butterfield, J., Bergman, J., Mershon, L., Rodionov, V., Vershinin, M., 2015. Cargo transport at microtubule crossings: evidence for prolonged tug-of-war between kinesin motors. Biophys. J. 108 (6), 1480–1483. doi:10.1016/j.bpj.2015.02.016.

Rai, A.K., Rai, A., Ramaiya, A.J., Jha, R., Mallik, R., 2013. Molecular adaptations allow dynein to generate large collective forces inside cells. Cell 152 (1–2), 172–182. doi:10.1016/j.cell.2012.11.044.

Schnitzer, M.J., Visscher, K., Block, S.M., 2000. Force production by single kinesin motors. Nat. Cell Biol. 2 (10), 718–723. doi:10.1038/35036345.

Shojania Feizabadi, M., Janakaloti Narayanareddy, B.R., Vadpey, O., Jun, Y., Chapman, D., Rosenfeld, S., Gross, S.P., 2015. Microtubule C-Terminal tails can change characteristics of motor force production. Traffic 16 (10), 1075–1087. doi:10.1111/tra.12307.

Soppina, V., Rai, A.K., Ramaiya, A.J., Barak, P., Mallik, R., 2009. Tug-of-war between dissimilar teams of microtubule motors regulates transport and fission of endosomes. Proc. Natl. Acad. Sci. USA 106 (46), 19381–19386. doi:10.1073/pnas.0906524106.

Srinivasan, M., Walcott, S., 2009. Binding site models of friction due to the formation and rupture of bonds: state-function formalism, force-velocity relations, response to slip velocity transients, and slip stability. Phys. Rev. E - Stat. Nonlinear Soft Matter Phys. 80 (4), 1–15. doi:10.1103/PhysRevE.80.046124.

Visscher, K., Schnitzer, M.J., Block, S.M., 1999. Single kinesin molecules studied with a molecular force clamp. Nature 400 (6740), 184–189. doi:10.1038/22146.

Walcott, S., 2008. The load dependence of rate constants. J. Chem. Phys. 128 (21), 215101. doi:10.1063/1.2920475.